

## ARTICLES

**Complex Phase Behavior in Aqueous Solutions of Poly(ethylene oxide)–Poly(ethylene) Block Copolymers****D. A. Hajduk,<sup>\*,†</sup> M. B. Kossuth, M. A. Hillmyer,<sup>‡</sup> and F. S. Bates\****Department of Chemical Engineering and Materials Science, University of Minnesota, Minneapolis, Minnesota 55455**Received: October 13, 1997; In Final Form: March 18, 1998*

The many similarities in morphological behavior exhibited by diblock copolymer melts and lyotropic surfactant suspensions suggest the existence of common physical principles underlying these phenomena. In an effort to identify such principles, we discuss the phase behavior of aqueous solutions of poly(ethylene oxide)–poly(ethylene) (PEO–PEE) block copolymers. The molecular weights of these materials are roughly twice that of common poly(ethylene oxide)–poly(propylene oxide) (PEO–PPO) surfactants, leading to microphase separation and a rich mesophase polymorphism in the absence of solvent. Despite the strongly thermotropic nature of the PEO–water interaction, the phase behavior in solutions of high polymer concentration is primarily lyotropic. Mesophase transitions observed in this regime show characteristics similar to those observed in undiluted block copolymers. A crossover to thermotropic behavior occurs at concentrations on the order of 60 wt % polymer, which corresponds to the formation of a stoichiometric complex of three water molecules per ethylene oxide repeat. This crossover is accompanied by changes in the structural dimensions, long-range order, and mechanical characteristics of the mesophases. Transitions in these dilute solutions resemble those previously observed in surfactant systems. These findings suggest that the complex structure of hydrated PEO plays a central role in determining the phase behavior of the system.

**Introduction**

It has long been recognized that the self-assembling behavior of block copolymers resembles that of aqueous solutions of amphiphiles in the liquid crystalline phases which are observed,<sup>1–12</sup> the sequences in which they appear,<sup>2,4,5</sup> and the epitaxial relations which connect these structures during morphological transformations.<sup>7,9,12–17</sup> The resulting structures have found widespread application in the preparation of mesoporous ceramics;<sup>18</sup> the synthesis of metal nanoparticles,<sup>19</sup> including semiconducting assemblies;<sup>20</sup> and the formation of microstructured polymeric gels.<sup>21</sup> Identification of the principles governing self-assembly in lyotropic liquid crystals would therefore have considerable implications for materials science. While the local structure of copolymers and amphiphiles permits certain superficial connections to be made (the microphase-separated interface in the block copolymer melt corresponds to the hydrophilic–hydrophobic interface in amphiphilic solutions), this structural homology is not reflected in the underlying microscopic interactions characteristic of each system, and the existence of a common origin for this behavior is far from certain.

Diblock copolymers represent an attractive model system for studies of amphiphilic self-assembly. These materials consist of two homopolymer chains (blocks) which are covalently

bonded together to create a single macromolecule. A repulsive interaction between the blocks produces a local phase separation at low temperatures, which leads to the formation of liquid crystalline phases (mesophases) in the absence of solvent. Theory suggests,<sup>22</sup> and experiment has shown,<sup>5,10</sup> that this behavior is universal when described in terms of the strength of the interactions between the blocks ( $\chi$ ), the total number of statistical segments ( $N$ ), the volume fraction of one of the blocks ( $f$ ), and differences in the conformational properties of the polymer chains ( $\epsilon$ ).<sup>23,24</sup> Since  $\chi$  depends on temperature, the resulting phase behavior is thermotropic. In contrast to conventional amphiphiles, the highly entangled nature of polymeric materials implies that segment–segment interactions are averaged over a large number of molecules, resulting in mean-field behavior at high molecular weights.<sup>25</sup> This facilitates the development of nonphenomenological theories, which in turn permits explicit connections to be established between microscopic and phenomenological descriptions of copolymer phase behavior.<sup>26–28</sup>

Most studies of melt state copolymer behavior have employed hydrocarbon-based materials such as polystyrene (PS) and polyisoprene (PI). Although the behavior of these materials in a selective solvent is weakly analogous to that of a conventional amphiphilic solution,<sup>29–33</sup> the complex local structure characteristic of aqueous solutions is absent. This can be remedied through the use of hydrophilic materials such as poly(ethylene oxide) (PEO). Recent publications have described synthetic schemes for several different amphiphilic copolymers,<sup>34–36</sup> and

\* To whom correspondence should be addressed.

<sup>†</sup> Current address: Symyx Technologies, 3100 Central Expressway, Santa Clara, CA 95051.

<sup>‡</sup> Current address: Department of Chemistry, University of Minnesota, Minneapolis, MN 55455.

**TABLE 1: Structural Characteristics of the PEO–PEE Copolymers<sup>a</sup>**

polymer	$f_{EO}$	$M_{n,EO}$ ( $Z_{EO}$ ) (g/mol)	$M_{n,EE}$ (g/mol)	$M_n$ (g/mol)	$M_w/M_n$	$\bar{N}$
OE-3	0.29	900 (20)	1600	2500	1.12	242
OE-1	0.34 <sup>b</sup>	1400 (32)	2000	3400	1.14	361
OE-7	0.39 <sup>b</sup>	1760 (40)	2140	3900	1.10	443
OE-6	0.42	2000 (46)	2100	4100	1.09	493
OE-8	0.42	1900 (43)	2000	3900	1.09	468
OE-4	0.44 <sup>b</sup>	2160 (49)	2140	4300	1.09	528
OE-9	0.46 <sup>b</sup>	2240 (51)	1960	4200	1.10	540
OE-2	0.48 <sup>b</sup>	1940 (44)	1660	3600	1.12	466
OE-12	0.52 <sup>b</sup>	1300 (29)	900	2200	1.11	306
OE-5	0.70	5000 (113)	3400	8400	1.09	1175
OE-10	0.72 <sup>b</sup>	5060 (152)	3640	8700	1.07	1196

<sup>a</sup>  $f_{EO}$ , PEO volume fraction.  $M_n$ , number-average molecular weight.  $M_w$ , weight-average molecular weight.  $Z_{EO}$ , degree of polymerization of the PEO block.  $\bar{N}$ , Ginsburg parameter for fluctuation corrections to mean-field theory for block copolymer melts,<sup>25</sup> calculated using structural data at 140 °C.<sup>44</sup> Molecular characteristics reported from ref 35. <sup>b</sup> Identifies polymers studied in aqueous solution.

copolymers of PEO and poly(propylene oxide) (PPO) are now commercially available. Such materials have found widespread application as emulsifiers, wetting agents, foam stabilizers, and detergents. Research has therefore tended to focus on their properties in solution.<sup>37–41</sup> Unfortunately, PPO is only weakly hydrophobic at low temperatures, and most PEO–PPO copolymers do not undergo microphase separation in the absence of solvent due to their low molecular weights. Commercial materials also possess significant polydispersities, which can complicate analysis of experimental data.

Recently, Hillmyer and Bates described the synthesis of a series of poly(ethylene oxide)–polyalkane (PEO–PA) diblock copolymers.<sup>35</sup> The polyalkane block can be formed from a variety of hydrogenated polyolefins to yield poly(ethylene) (PEE), poly(ethylene-*co*-propylene) (PEP), or polyethylene (PE), and the use of anionic polymerization techniques generates nearly monodisperse materials with well-defined compositions. Such polymers may be viewed as the macromolecular equivalent of the well-known alkane–oxyethylene ( $C_nEO_m$ ) surfactants (here,  $n \approx 160$  and  $m \approx 50$ ) in which crystallization of the alkane block is hindered by the presence of ethyl branches. In contrast to the commercially available PEO–PPO materials, the highly incompatible nature of these segments ( $\chi_{EO-EE} \approx 1$  at 100 °C)<sup>42</sup> produces microphase separation at relatively modest molecular weights. This results in a rich mesophase polymorphism<sup>43</sup> which matches that observed in block copolymers of much higher molecular weight, suggesting that mean-field theory provides an accurate description of the melt state phase behavior. Here, we exploit the presence of a hydrophilic block to move continuously from the thermotropic behavior characteristic of undiluted block copolymers to the lyotropic behavior characteristic of amphiphiles. Using small-angle X-ray scattering, we describe the phase behavior of these materials as a function of concentration and temperature and identify the structural changes that result upon the addition of water.

## Experimental Section

Synthesis and characterization of the PEO–PEE copolymers have been described in detail elsewhere.<sup>35</sup> The molecular characteristics are summarized in Table 1. The modestly broadened molecular weight distributions (indexed by  $M_w/M_n$ , where  $M_w$  is the weight-average molecular weight and  $M_n$  is the number-average molecular weight of these anionically synthesized polymers) reflect the low degree of polymerization

of both blocks; however, these values compare favorably with commercially available PEO–PPO materials.

Viscoelastic characteristics of unsolvated copolymers were measured on a Rheometrics RSA-II rheometer using a shear sandwich geometry in oscillatory mode with a sample thickness of 0.5 mm. A nitrogen purge was used to minimize oxidative degeneration at high temperatures. Copolymers were melted at 50 °C and placed on the rheometer plates. After the gap thickness was adjusted, excess material was removed, and the polymer was permitted to recrystallize at 10 °C prior to beginning measurements. This resets the sample morphology to a randomly oriented, semicrystalline lamellar phase, minimizing the effect of nonequilibrium morphologies arising from sample preparation. The dynamic elastic ( $G'$ ) and loss ( $G''$ ) moduli were monitored at a frequency of 1.0 rad/s and a strain amplitude of 1% while being heated at 1 °C/min. Discontinuities in  $G'(T)$  were used to detect transitions between different ordered morphologies which were then analyzed in detail using small-angle scattering techniques.

Melt samples for scattering measurements were prepared by melt pressing at 50 °C, followed by crystallization of the PEO block at room temperature. Solution samples were prepared by placing measured amounts of copolymer and high-purity deionized water in acid-washed quartz capillaries 1.5 mm in outer diameter and sealing with a column of commercial five-minute epoxy. Estimates of the amount of water absorbed by the epoxy seal suggest that the resulting uncertainty in concentration is negligible except for the most concentrated solutions (above 85 wt % polymer); these uncertainties have been included in the error limits reported here. Samples were homogenized through a combination of repeated centrifugation, thermal cycling across the melting point of the PEO block, and extended annealing at moderate temperatures. Homogenization was confirmed directly through optical birefringence measurements and indirectly by comparing structural measurements made at six-week intervals. Size exclusion chromatography (SEC) performed after structural characterization revealed negligible degradation of the copolymer.

Small-angle X-ray scattering (SAXS) measurements were conducted on a small-angle beamline constructed at the University of Minnesota. Cu K $\alpha$  X-rays were generated by a Rigaku RU-200BVH rotating anode X-ray machine equipped with a 0.2  $\times$  2 mm microfocus cathode and Franks mirror optics. Samples were placed inside an evacuated sample chamber and maintained at the appropriate temperature by a pair of heaters mounted on a water-cooled brass block (temperature range 5–260 °C, stability  $\pm 0.1$  °C). Solutions were limited to an upper temperature limit of 80 °C in order to minimize both the degradation of the PEO chains and the possibility of seal failure due to the increase in pressure inside the capillary. Two-dimensional diffraction images were collected with a multiwire area detector (HI-STAR, Siemens Analytical X-ray Instruments) and corrected for detector response characteristics prior to analysis. Typical exposure times ranged from 30 to 300 s. Images were converted to a one-dimensional format by integrating azimuthally along an arc  $\pm 30^\circ$  about a direction normal to the capillary axis.

Diffraction from semicrystalline lamellar morphologies (X), consisting of crystalline PEO and amorphous PEE layers, exhibited only a few broad reflections at spacing ratios of 1:2:3; see Figure 1. Diffraction from lamellar (L) phases was characterized by peaks at spacing ratios of 1:2:3:4... Diffraction from cylindrical phases exhibited peaks characteristic of a hexagonal packing at ratios of  $1:\sqrt{3}:\sqrt{4}:\sqrt{7}:\sqrt{9}$ ... In block

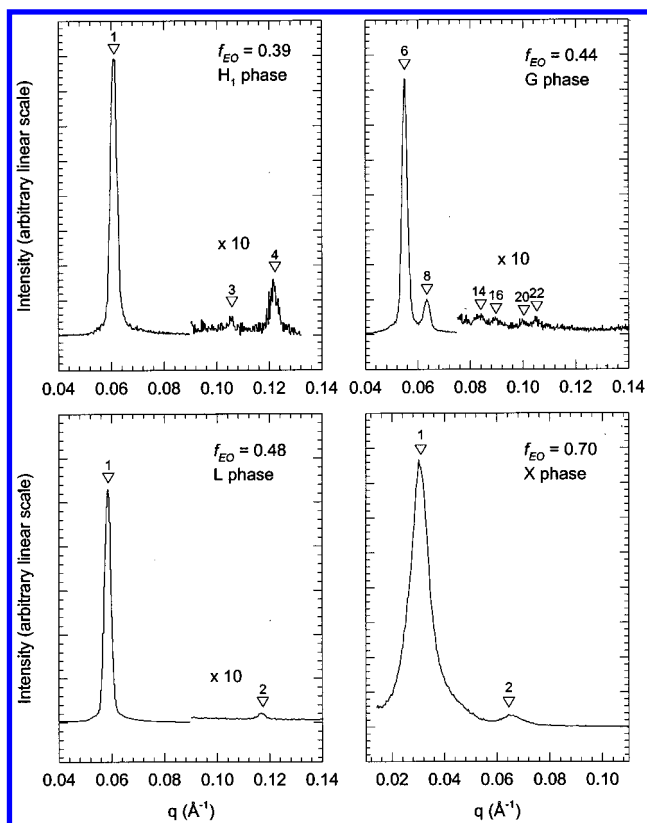


**Figure 1.** Representative melt state diffraction from four of the copolymers used in this study. Inverted triangles mark the positions of the expected reflections for the indicated morphology. Each curve required between 120 and 180 s of integration.

copolymer melts, such phases are commonly denoted C, for cylindrical; in this work, we adopt the amphiphilic notation H, for hexagonal. These phases are further subdivided into type 1 (H<sub>1</sub>, “normal”, or “oil-in-water”), with cylinders of PEE in a PEO matrix, and type 2 (H<sub>2</sub>, “inverted”, or “water-in-oil”), with cylinders of PEO in a PEE matrix. The former can, in principle, exhibit an infinite degree of swelling; the latter cannot. Since small-angle scattering cannot differentiate between H<sub>1</sub> and H<sub>2</sub> phases (Babinet’s principle), the assignment was made on the basis of the volume fraction of PEE in solution. Scattering from H<sub>1</sub> phases in dilute solution frequently exhibited a broad maximum at positions corresponding to the first peak in the form factor for an isolated, infinitely long cylinder of the appropriate radius. The presence of this maximum provided additional confirmation of the cylindrical microstructure. Diffraction from the bicontinuous gyroid (G<sub>1</sub>, G<sub>2</sub>) morphology, of space group *Ia* $\bar{3}$ *d*, was characterized by reflections at ratios of  $\sqrt{6}:\sqrt{8}$ , with a relative intensity ratio of approximately 10:1, as is commonly observed in neat block copolymers. Higher order reflections were occasionally observed at positions characteristic of the *Ia* $\bar{3}$ *d* space group.

Interfacial area per chain (*A*) was determined geometrically from the repeat spacing of the mesophase (*d*), measured via SAXS; the volume fraction of the unit cell occupied by the poly(ethylene) (PEE) block ( $\phi$ ), calculated from the solution stoichiometry; and the volume of the PEE block (*V*), calculated from NMR measurements of the polybutadiene precursor, as described in ref 35. For the lamellar (L) phase,

$$A = \frac{V}{\phi d} \quad (1)$$

for the normal hexagonal (H<sub>1</sub>) phase,

$$A = \frac{2V}{R}, \quad R = \sqrt{\frac{2\phi}{\pi\sqrt{3}}}d \quad (2)$$

and for the inverted hexagonal (H<sub>2</sub>) phase,

$$A = \frac{2V(1/\phi - 1)}{R}, \quad R = \sqrt{\frac{2(1 - \phi)}{\pi\sqrt{3}}}d \quad (3)$$

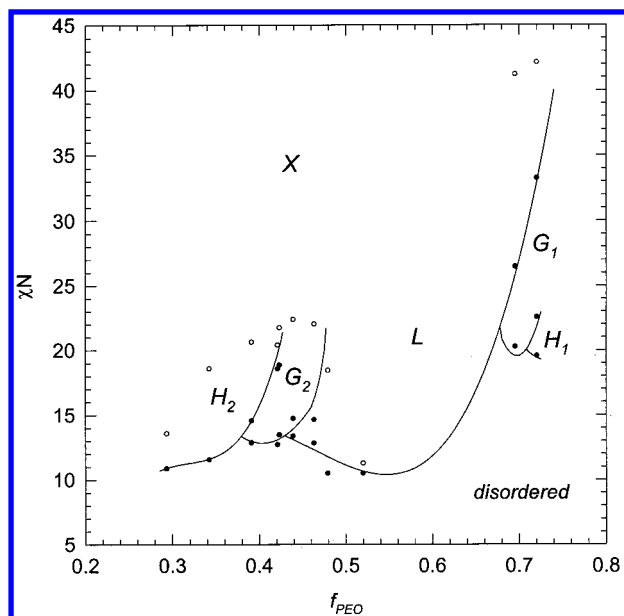
For both of the hexagonal phases, *R* is the cylinder radius, and the repeat spacing (*d*) is related to the intercylinder spacing (*a*) through  $a = 2/\sqrt{3} d$ .

Estimation of the area for the normal and inverted (G<sub>1</sub> and G<sub>2</sub>) gyroid phases was performed by assuming that the spacing of the G [211] plane was equal to the lamellar repeat spacing, as suggested by Figure 4, and then employing a constant mean curvature approximation to the G minimal surface to calculate the total interfacial area within the unit cell.<sup>59</sup> Dividing this value by the number of polymer chains in the unit cell yielded an estimate for *A*. This should not be taken to imply that the actual PEO-PEE interface possesses constant mean curvature, however.<sup>27,46,47</sup>

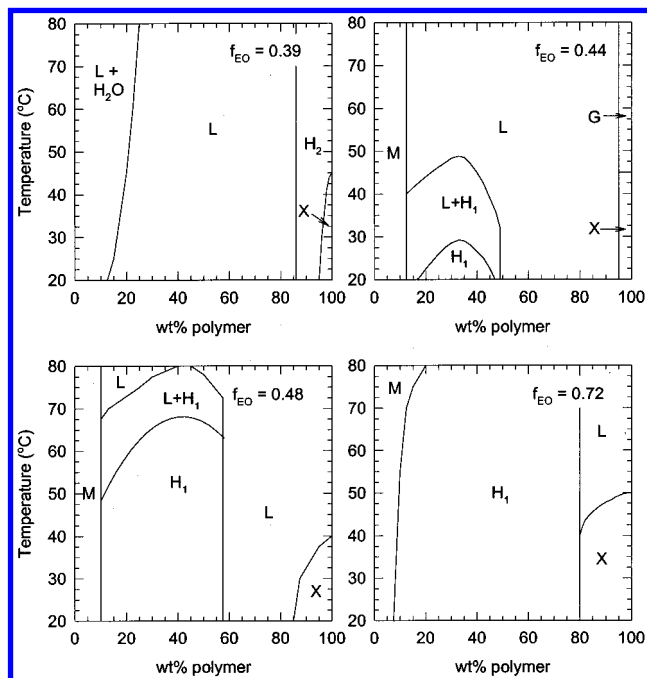
## Results

Figure 2 displays the ordered state morphologies identified after prolonged annealing in the absence of solvent. All of the copolymers adopt a semicrystalline lamellar morphology (X) at low temperatures, as evidenced by two relatively broad diffraction peaks at a reciprocal space position ratio of 1:2. When heated above the melting point of the PEO domains, copolymers with *f*<sub>EO</sub> of 0.48 or greater form lamellar phases (L), while those with *f*<sub>EO</sub> of 0.39 or less form hexagonally packed cylinders of PEO in a PEE matrix (H<sub>2</sub>). The materials with *f*<sub>EO</sub> = 0.42, 0.44, and 0.46 initially produced two sets of reflections at positions characteristic of coexisting lamellar (L) and hexagonally packed cylindrical (H<sub>2</sub>) phases before eventually transforming to the gyroid (G<sub>2</sub>) phase. This presumably reflects the relaxation of a nonequilibrium lamellar structure which was produced at low temperatures by the crystallization of the PEO domains. In amphiphilic systems, intermediate cylindrical (H<sub>1</sub>) phases have been observed during the L → G transition. However, this L + H<sub>2</sub> diffraction is equally consistent with a hexagonally perforated layer phase,<sup>5</sup> in which hexagonally packed channels of the majority component material (PEE) extend through alternating layers of minority (PEO) and majority (PEE) component material. In block copolymers, perforated layer (PL) morphologies occur as nonequilibrium structures during the L → G transformation;<sup>10</sup> some evidence exists for their appearance in amphiphiles as well.<sup>11,12</sup>

The solubility of these molecules in water depends strongly on their PEO content. Polymers with *f*<sub>EO</sub> ≤ 0.34 are essentially immiscible in water. In the melt, these materials formed H<sub>2</sub> phases; we speculate that hydration of the PEO domains introduces sufficient variation into the mean thickness of the PEE layer to destabilize the swollen morphology. Such “packing frustration” governs the swelling of H<sub>2</sub> phases in conventional surfactants<sup>45,46</sup> and stabilizes the bicontinuous cubic phases in both copolymers and amphiphiles.<sup>27,46–48</sup> Phase inversion is apparently precluded in this case by the restrictions this would place on the conformations of the PEE and PEO chains. Polymers with *f*<sub>EO</sub> = 0.39 adopt the H<sub>2</sub> phase in concentrated solution but transform to the L phase upon dilution before separating into coexisting lamellar and bulk water phases. Polymers containing higher fractions of PEO form liquid crystal



**Figure 2.** PEO-PEE copolymer phase behavior in the absence of solvent as a function of the PEO volume fraction ( $f_{\text{PEO}}$ ) and the degree of segregation ( $\chi N \approx 1/T$ ). Data points are shown in black; the phase boundaries shown are guides to the eye. Open symbols identify the melting temperature of the PEO block, which corresponds to the highest segregation at which measurements can be made. The symbols identify different liquid crystalline phases: X, semicrystalline lamellae; L, amorphous lamellae; H, hexagonally packed cylinders; G, gyroid. The subscripts identify these phases as "PEE in PEO" (type 1) or "PEO in PEE" (type 2). A spatially isotropic phase in which PEO and PEE mix freely is observed at low segregations (high temperatures). The asymmetry of the diagram about  $f_{\text{PEO}} = 0.5$  reflects the conformational asymmetry of these two polymers.



**Figure 3.** Experimental phase diagrams for four of the copolymers in the concentration-temperature plane. Phase boundaries were identified to within at least 2.5 °C in temperature and 5 wt % polymer in composition.

phases over a wide range of concentrations and temperatures; an optically isotropic micellar solution appears at the highest water contents.

Figure 3 summarizes the mesophases observed in selected materials as a function of concentration and temperature. The

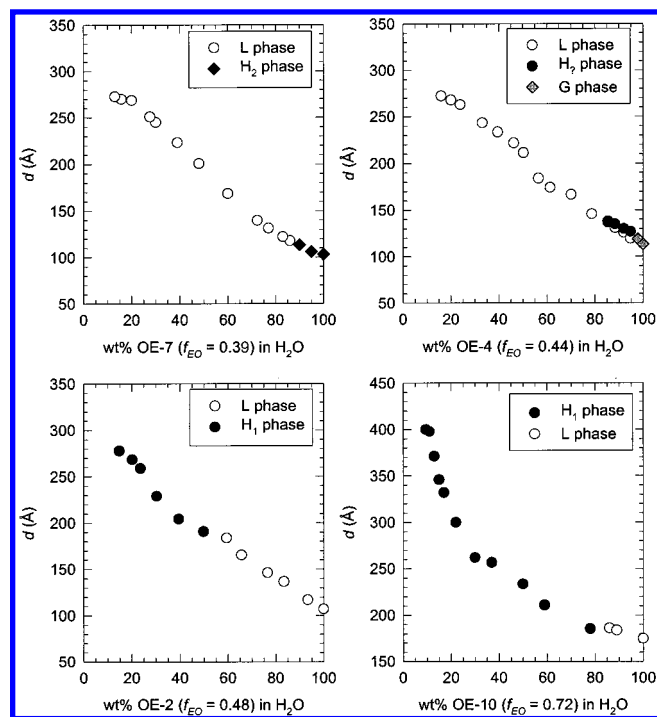


**Figure 4.** Lowest order repeat spacing for four of the copolymers as a function of concentration at 50 °C. Qualitatively identical curves were obtained for the other copolymers. The uncertainties in these numbers are less than 2%.

polymeric nature of the hydrophilic and hydrophobic chains permits us to adjust the "hydrophobic-lipophilic balance"—parametrized here by  $f_{\text{EO}}$ , the volume fraction of the hydrophilic block—to a far higher degree of precision than is possible in conventional surfactants. Although it is not obvious that these findings can be reduced to a single universal diagram, the data show a systematic decrease in the fraction of each diagram occupied by the L morphology as the PEO content increases. This decrease is only weakly correlated with the reduction in the volume fraction of the hydrophobic domain. Surprisingly, despite the strongly thermotropic nature of the PEO-water interaction,<sup>49</sup> the phase behavior is lyotropic except in the most dilute solutions. In combination with the absence of two-phase regions, this suggests that the concentrated solution phase behavior is dominated by effects associated with the hydration of PEO.

Structural measurements are consistent with the view that the complex PEO-water interaction governs the phase behavior. In the water-soluble systems, both the lowest order repeat spacing (Figure 4) and the interfacial area per chain (Figure 5) increase upon hydration. At a concentration of about 10 wt % water, compositionally asymmetric materials ( $f_{\text{EO}} \neq 0.5$ ) transform to a new ordered morphology which is accompanied by a substantial reduction in the interfacial area per chain. The repeat spacing ( $2\pi/q^*$ , where  $q^*$  is the position of the lowest order Bragg reflection) is continuous across the transition, consistent with findings in other block copolymers<sup>7,17</sup> and some,<sup>50</sup> but not all,<sup>11,51-53</sup> surfactants. After the new structure is formed, the repeat spacing increases continuously upon dilution while the interfacial area per chain remains essentially constant. Diffraction from samples in this region shows multiple higher order reflections indicative of mesophases with well-developed long-range order.

Upon further dilution, the interfacial area per chain increases rapidly without producing a discontinuity in the concentration dependence of the repeat spacing. At the same time, the

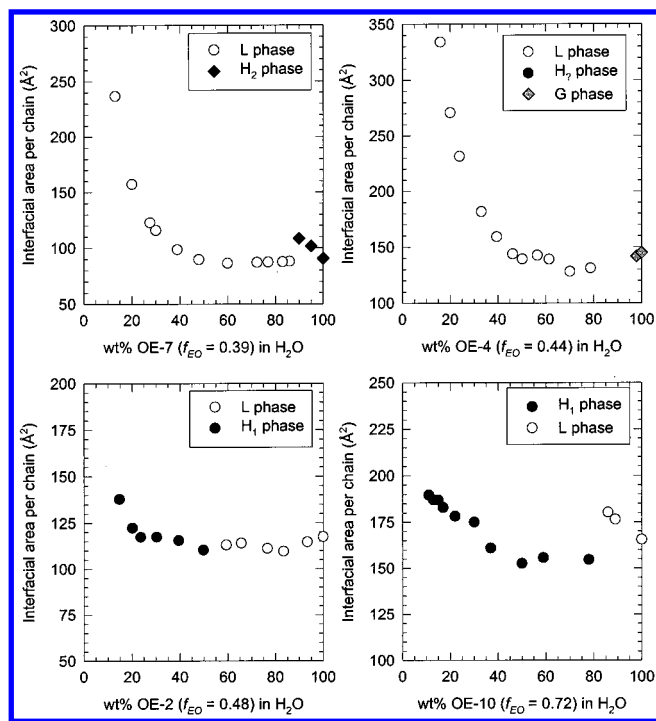


**Figure 5.** Interfacial area per PEO-PEE junction for four of the copolymers as a function of concentration at 50 °C. In the asymmetric copolymers, the rapid increase in area occurs at a concentration of about three water molecules per EO unit. Error bars for these values are concealed by the symbols.

solutions turn cloudy. Small-angle scattering does not show any evidence of a second ordered morphology, and extended centrifugation or prolonged annealing does not result in macrophase separation. We speculate that this turbidity reflects the presence of lattice defects with correlation lengths comparable to the wavelength of light. Consistent with this interpretation, the degree of long-range order in the system (as measured by the increase in diffraction peak width as a function of  $q$ ) decreases markedly at this time (Figure 6). The sudden appearance of these defects presumably indicates a significant change in the elastic characteristics of the mesophases.

At this point, order-order transitions were observed as functions of both water concentration and temperature in solutions of the most symmetric copolymers ( $f_{EO} = 0.44, 0.46, 0.48$ , and  $0.52$ ). Upon heating, the samples transformed from a normal hexagonal phase ( $H_1$ ) at low temperatures, through coexisting lamellar and hexagonal phases, to a poorly ordered lamellar morphology (L) at high temperatures (Figure 7). Cooling the solutions returned the samples to well-ordered hexagonal phases, as expected. As in concentrated solutions, the domain spacings for coexisting lamellar and hexagonal phases agreed to within 2–3%; again, such correlations are commonly observed in copolymers but are somewhat less common in small-molecule surfactants. Since both the lamellar and hexagonal morphologies produce reflections at integral spacing ratios, such coexistence was identified through temperature-dependent changes in the relative intensities of the higher order diffraction peaks (when heating from the  $H_1$  phase) or through the appearance of noninteger reflections (when cooling from the L phase). Neither extended annealing in the vicinity of these transitions nor repeated thermal cycling across these transitions<sup>54</sup> resulted in the formation of cubic phases.

At the highest water contents, solutions of the material with  $f_{EO} = 0.39$  exhibited macrophase separation into a polymer-rich phase with diffraction characteristic of a poorly ordered

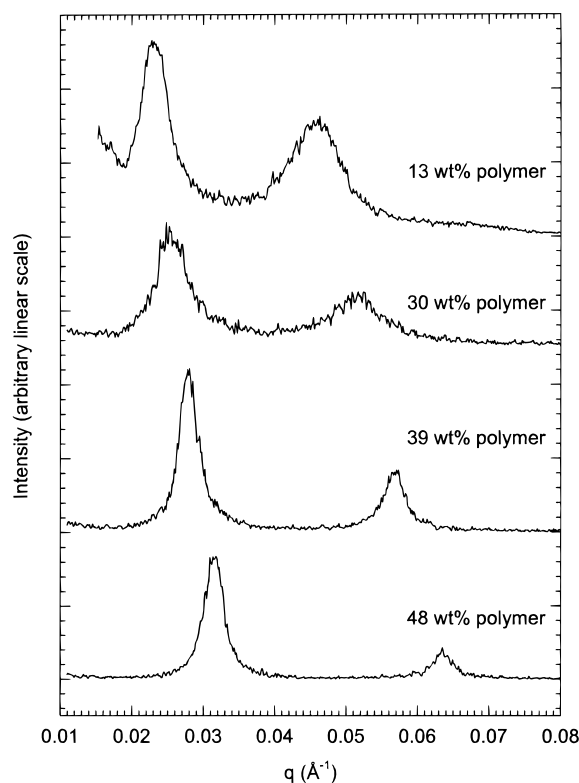


**Figure 6.** Diffraction from the  $f_{EO} = 0.39$  copolymer at 50 °C as a function of water concentration. Reflections occur at a position ratio of 1:2, characteristic of a lamellar phase. Upon dilution, the increase in both the width of the diffraction reflections and the rate at which this width increases with  $q$  signals a loss of long-range order.

lamellar phase and into a polymer-poor phase which was optically isotropic and did not produce any small-angle X-ray signature. The repeat spacing of this dilute lamellar phase was independent of concentration. Dilute solutions of the other copolymers experienced a transition from a poorly ordered mesophase to a new structure characterized by only a single, broad X-ray reflection, suggestive of a liquidlike micellar dispersion. The location of these transitions was strongly dependent on both the concentration and the temperature of the solutions. Further analysis of the micellar phases will be described in a separate report.

## Discussion

The phase behavior of the polymeric solutions resembles that observed in the short-chain polyalkane-poly(oxyethylene) ( $C_nEO_m$ ) surfactants in terms of the mesophases that are observed, the sequence in which they appear as a function of concentration, and the evolution of the phase behavior as a function of molecular composition. Many of the differences between these systems, such as the high melting temperature of the PEO domains (Krafft temperature) and the absence of a molecularly dispersed phase from the copolymer diagrams, can be traced to the higher molecular weights of the polymeric materials. This also affords a far greater degree of control over the “hydrophilic-lipophilic balance” of the surfactant than is possible in the  $C_nEO_m$  systems; in the latter, addition or removal of a single methylene or ethylene oxide unit produces dramatic changes in phase behavior.<sup>55</sup> Finally, the experimentally measured melt state phase diagram (Figure 2) agrees with that predicted by the mean-field solution of the self-consistent field theory for block copolymer melts<sup>22–24</sup> in the mesophases which are observed, the sequences in which they appear, the composi-



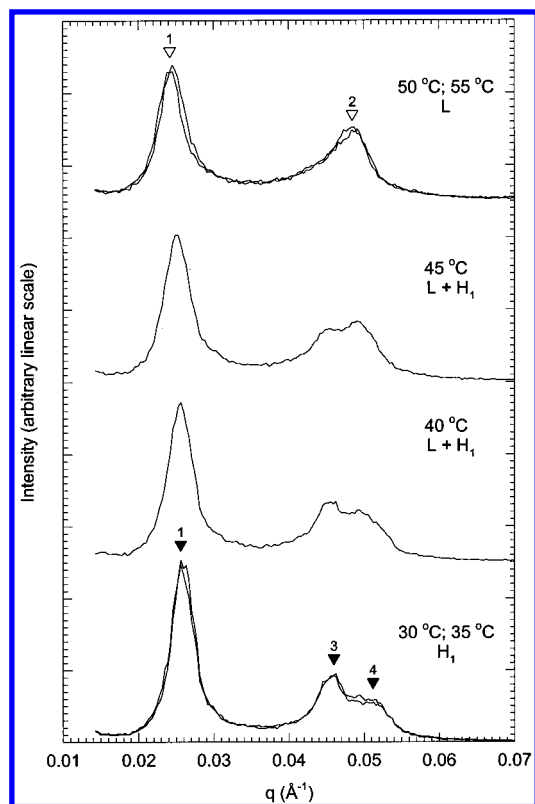


**Figure 7.**  $H_1 \rightarrow L$  transition sequence observed upon heating 28 wt % of the  $f_{EO} = 0.46$  copolymer.  $H_1$  and  $L$  reflections are indicated by filled and open symbols, respectively. Since the first-order peak positions of the two morphologies coincide, changes in the relative intensities of the higher order reflections were used to identify temperatures at which the two phases coexist. These intensities are essentially independent of temperature for the pure  $H_1$  and  $L$  phases, as shown by the superposition of profiles recorded at 30 and 35 °C, and 50 and 55 °C. Cooling the solution returns it to the  $H_1$  phase, as expected.

tions at which they appear, and the compositional asymmetry of the overall diagram. This suggests that these PEO-PEE copolymers retain their polymeric character even at molecular weights of approximately 4000 g/mol. Preliminary analysis of the solution phase behavior can therefore be performed using concepts developed in block copolymers.

Mesophases are stabilized in copolymer melts by competition between the interfacial and conformational contributions to the free energy of the chains. The former arises from the contact interaction between chemically dissimilar segments and drives the system to minimize the interfacial area of the morphology; the latter is entropic in origin and drives the blocks to adopt random coil conformations. At low temperatures, water is a strongly preferential solvent for PEO; estimates of the heat of dilution per monomer ( $h$ ) indicate that  $h_{PEO-H_2O} \approx -0.7$  kT at 25 °C,<sup>56</sup> whereas  $h_{PEE-H_2O} \approx 5$  kT.<sup>57</sup> This disparity suggests that all of the water is located in the PEO domains and that very little mixing of PEO and PEE segments occurs across the interface separating them, i.e., that the blocks are strongly segregated. Although this implies that the chains are highly stretched normal to the PEO-PEE interface, the strength of the PEE-water interaction might induce the PEO chain to collapse against this interface in order to screen out energetically unfavorable PEE-water contacts. The specific volume of amorphous PEO can be estimated from published data to be 64 Å<sup>3</sup> per EO at 20 °C.<sup>58</sup> Assuming a length per EO of 3.6 Å, between 6 and 10 monomers (about 20% of the PEO block in the PEE-rich copolymers) must locate at the PEO-PEE interface

in order to completely shield the hydrophobic domain in most of the solutions (see Figure 3). Such an arrangement would entail a significant and physically unlikely loss of conformational entropy. However, it is certainly possible that a modest degree of screening occurs.

Such segregation accounts for the near-complete absence of the gyroid (G) phase from the experimentally measured phase diagrams. In both amphiphilic suspensions and block copolymer melts, the phase frequently appears at compositions and temperatures separating the lamellar (L) and cylindrical (C,  $H_1$ , or  $H_2$ ) morphologies. In the solutions examined here, structural measurements at the  $L-H_1$  and  $L-H_2$  boundaries suggest that the interfacial area per chain in the  $G_1$  and  $G_2$  phases, respectively, lies between the values for the lamellar and cylindrical morphologies.<sup>59</sup> Formation of the gyroid would therefore reduce the interfacial contribution to the free energy of the system; its absence from the experimental diagrams must therefore be due to conformational effects. Theory indicates that although the morphology is stable in weakly segregated copolymers, it is destabilized in strongly segregated copolymer melts by packing frustration in both the minority and majority component domains.<sup>27</sup> Similar considerations influence its stability in amphiphilic systems.<sup>46-48</sup> The rapid disappearance of the  $G_2$  phase upon hydration of  $G_2$ -forming copolymer melts (Figure 1)—that is, upon moving from weak to strong segregation—is consistent with this view.

We hypothesize that the structural aspects of this phase behavior are closely associated with changes in the conformational properties of PEO. Studies of PEO conformations indicate that the polymer forms a random coil in the melt (via SANS<sup>58</sup>) and in aqueous solution (via dilute solution light scattering,<sup>60</sup> viscometry,<sup>61-64</sup> and electron spin resonance<sup>65</sup>). In the melt, the backbone of the chain adopts a locally disordered structure. In aqueous solution, it is unclear whether the chain assumes a completely disordered local structure, a poorly ordered structure, or a helical conformation similar to that seen in the crystalline state. Recent numerical simulations<sup>66</sup> suggest that the molecule assumes an 11/2 helix in aqueous solution with a pitch of  $16 \pm 3$  Å.

The conformational flexibility of the molecule changes dramatically upon hydration. For a polymer with  $M_w = 10^6$  g/mol,  $R_g$  at 20 °C rises from 366 Å in the melt to 566 Å in water.<sup>60</sup> Statistical segment lengths may be estimated by applying a wormlike chain model in which the contour length  $L$  is given by  $Nb$ , where  $N$  is the number of segments of length  $b$ . Assuming a backbone length per EO repeat unit of 3.6 Å,  $b$  rises from 9.8 Å (2.7 EO units) in the melt to 29 Å (8 EO units) in aqueous solution with locally disordered conformations or 40 Å (13.6 EO units, 2.5 turns) with locally helical conformations. In systems of low molecular weight such as the PEO-PEE copolymers examined here, the associated drop in the number of segments might alter the statistical character of the polymer, producing a transition from “random coil” to nearly “rodlike” conformations. This is supported by intrinsic viscosity measurements, which show departures from the high molecular weight response for chains with molecular weights below ca. 5000 g/mol.<sup>67</sup>

Calorimetric measurements indicate that the PEO-water interaction is characterized by a relatively high heat of dilution and a negative entropy of mixing.<sup>49,56,68,69</sup> Since the change in free energy associated with hydration of PEO greatly exceeds that arising from changes in the internal conformations of the polymer chains, this interaction effectively imposes a constraint on the concentration of water within the PEO domains and, thus,

on the interfacial tension associated with the (hydrated PEO)-PEE interface. The large change in interfacial area per chain associated with the lyotropic transitions in concentrated solutions (Figure 5) and the absence of two-phase regions from the polymer-rich regions of the experimentally measured phase diagrams (Figure 3) are consistent with this view.

The negative entropy of mixing reflects the formation of a stoichiometric complex of between two and four water molecules per EO;<sup>66,70-73</sup> further dilution does not affect the local environment of the EO segments. The conformational change discussed above may be associated with the formation of this complex; confirmation of this hypothesis would require data on PEO conformations in concentrated solution, which are at present unavailable. The concentration range within which this complex forms corresponds to the point at which the interfacial area per molecule begins to increase rapidly (Figure 5); the solutions become turbid, suggesting a change in the elastic characteristics of the mesophases; and thermotropic transitions are first observed (Figure 7). That is, full hydration of the PEO chain is associated with a crossover from lyotropic to thermotropic behavior.

## Conclusions

Macromolecular amphiphiles such as the poly(ethylene oxide)-polyethylethylene (PEO-PEE) diblock copolymers examined here possess several important advantages over the short-chain nonionic surfactants ( $C_nEO_m$ ) conventionally used for experimental studies of self-assembly. Due to the high molecular weights and mutually immiscible nature of the PEO and PEE blocks, these materials undergo microphase separation in the absence of solvent, resulting in a phase behavior that matches that observed in copolymers of much greater molecular weight. Insights developed in studying the latter class of materials might be profitably extended to these polymeric amphiphiles.

Upon addition of water, this thermotropic mesomorphism evolves continuously into the lyotropic behavior characteristic of the short-chain amphiphiles, with thermotropic transitions reappearing in the most dilute solutions. Compared to the latter, the high molecular weights of the PEO and PEE blocks stabilize liquid crystalline morphologies over a substantially larger fraction of the resulting phase diagrams. They also facilitate precise control of the "hydrophilic-lipophilic balance", thereby highlighting the dependence of this polymorphism on the molecular composition. The disappearance of the gyroid morphology from the solution phase diagrams is explained by the highly stretched conformations adopted by the chains upon hydration of the PEO block.

Structural measurements indicate that many features of the phase diagrams reflect the formation of a stoichiometric complex of approximately three water molecules per EO, in reasonable agreement with previous studies. At lower solvent concentrations, the change in free energy associated with hydration of PEO dominates that associated with variation in interfacial area or molecular conformations, resulting in lyotropic behavior and the absence of two-phase windows. At higher concentrations, the strongly thermotropic nature of the PEO-water interaction leads to thermotropic transitions between different ordered mesophases. Regions of two-phase coexistence are also seen. Formation of this complex is presumably associated with a change in the conformational characteristics of the PEO block, which might best be viewed as a transition from "coil-coil" to "rod-coil" behavior. Preliminary results from studies of the same copolymers in solutions of oligomeric poly(ethylene

glycol) ( $M_w \approx 106$  g/mol) are strikingly different: although the trends in repeat spacing and interfacial area per chain are reminiscent of those seen in aqueous solution, only a lamellar structure is observed, regardless of amphiphile concentration and temperature.

**Acknowledgment.** Support for this work was provided by the National Science Foundation (DMR-9405101) and by the Center for Interfacial Engineering at the University of Minnesota.

## References and Notes

- (1) Seddon, J. M. *Biochim. Biophys. Acta* **1990**, 1031, 1.
- (2) Seddon, J. M.; Templer, R. H. *Philos. Trans. R. Soc. London A* **1993**, 344, 377.
- (3) Matsen, M. W.; Schick, M. *Curr. Opin. Colloid Interface Sci.* **1996**, 1, 329.
- (4) Fontell, K. *Colloid Polym. Sci.* **1990**, 268, 264.
- (5) Bates, F. S.; Schulz, M. F.; Khandpur, A. K.; Förster, S.; Rosedale, J. H.; Almdal, K.; Mortensen, K. *Faraday Discuss.* **1994**, 98, 7.
- (6) Hajduk, D. A.; Harper, P. E.; Gruner, S. M.; Honeker, C. C.; Kim, G.; Thomas, E. L.; Fetters, L. J. *Macromolecules* **1994**, 27, 4063.
- (7) Schulz, M. F.; Bates, F. S.; Almdal, K.; Mortensen, K. *Phys. Rev. Lett.* **1994**, 73, 86.
- (8) Hajduk, D. A.; Harper, P. E.; Gruner, S. M.; Honeker, C. C.; Thomas, E. L.; Fetters, L. J. *Macromolecules* **1995**, 28, 2570.
- (9) Hamley, I. W.; Koppi, K. A.; Rosedale, J. H.; Bates, F. S.; Almdal, K.; Mortensen, K. *Macromolecules* **1993**, 26, 5959.
- (10) Hajduk, D. A.; Takenouchi, H.; Hillmyer, M. A.; Bates, F. S.; Vigild, M. E.; Almdal, K. *Macromolecules* **1997**, 30, 3788.
- (11) Burgoyne, J.; Holmes, M. C.; Tiddy, G. J. T. *J. Phys. Chem.* **1995**, 99, 6054.
- (12) Fairhurst, C. E.; Holmes, M. C.; Leaver, M. S. *Langmuir* **1996**, 12, 6336.
- (13) Raçon, Y.; Charvolin, J. *J. Phys. Chem.* **1988**, 92, 2646.
- (14) Raçon, Y.; Charvolin, J. *J. Phys. Chem.* **1988**, 92, 6339.
- (15) Clerc, M.; Levelut, A. M.; Sadoc, J. F. *J. Phys. II* **1991**, 1, 54.
- (16) Sakurai, S.; Kawada, H.; Hashimoto, T.; Fetters, L. J. *Macromolecules* **1993**, 26, 5796.
- (17) Förster, S.; Khandpur, A. K.; Zhao, J.; Bates, F. S.; Hamley, I. W.; Ryan, A. J.; Bras, W. *Macromolecules* **1994**, 27, 6922.
- (18) Antonelli, D. M.; Ying, J. Y. *Curr. Opin. Colloid Interface Sci.* **1996**, 1, 523, and references therein.
- (19) Puvvada, S.; Baral, S.; Chow, G. M.; Qadri, S. B.; Ratna, B. R. *J. Am. Chem. Soc.* **1994**, 116, 2135.
- (20) Braun, P. V.; Osenar, P.; Stupp, S. I. *Nature* **1996**, 380, 325.
- (21) Desai, S. D.; Gordon, R. D.; Gronda, A. M.; Cussler, E. L. *Curr. Opin. Colloid Interface Sci.* **1996**, 1, 519.
- (22) Matsen, M. W.; Bates, F. S. *Macromolecules* **1996**, 29, 1091, and references therein.
- (23) Vavasour, J. D.; Whitmore, M. D. *Macromolecules* **1992**, 25, 5477.
- (24) Matsen, M. W.; Schick, M. *Macromolecules* **1994**, 27, 4014.
- (25) Fredrickson, G. H.; Heland, E. *J. Chem. Phys.* **1987**, 87, 697.
- (26) Hajduk, D. A.; Gruner, S. M.; Rangarajan, P.; Register, R. A.; Fetters, L. J.; Honeker, C.; Albalak, R. J.; Thomas, E. L. *Macromolecules* **1994**, 27, 490.
- (27) Matsen, M. W.; Bates, F. S. *Macromolecules* **1996**, 29, 7641.
- (28) Matsen, M. W.; Bates, F. S. *J. Chem. Phys.* **1997**, 106, 1.
- (29) Balsara, N. P.; Tirrell, M.; Lodge, T. P. *Macromolecules* **1991**, 24, 1975.
- (30) Tuzar, Z.; Kratochvil, P. In *Surface and Colloid Science*; Matijevic, E., Ed.; Plenum Press: New York, 1993; Vol. 15.
- (31) Lodge, T. P.; Xu, X.; Ryu, C. Y.; Hamley, I. W.; Fairclough, J. P. A.; Ryan, A. J.; Pedersen, J. S. *Macromolecules* **1996**, 29, 5955.
- (32) McConnell, G. A.; Gast, A. P. *Macromolecules* **1997**, 30, 435.
- (33) Hamley, I. W.; Fairclough, J. P. A.; Ryan, A. J.; Ryu, C. Y.; Lodge, T. P.; Gleeson, A. J.; Pedersen, J. S. *Macromolecules* **1998**, 31, 1188.
- (34) Qin, A.; Tian, M.; Ramireddy, S.; Webber, S. E.; Munk, P.; Tuzar, Z. *Macromolecules* **1994**, 27, 120.
- (35) Hillmyer, M. A.; Bates, F. S. *Macromolecules* **1996**, 29, 6994.
- (36) Mai, S.-M.; Fairclough, J. P. A.; Hamley, I. W.; Matsen, M. W.; Denney, R. C.; Liao, B.-X.; Booth, C.; Ryan, A. J. *Macromolecules* **1996**, 29, 6212.
- (37) Alexandridis, P.; Olsson, U.; Lindman, B. *Langmuir* **1996**, 12, 1419.
- (38) Wanka, G.; Hoffman, H.; Ulbricht, W. *Macromolecules* **1994**, 27, 4145.
- (39) Malmsten, M.; Linse, P.; Zhang, K.-W. *Macromolecules* **1993**, 26, 2905.
- (40) Alexandridis, P. *Curr. Opin. Colloid Interface Sci.* **1996**, 1, 490.

- (41) Noolandi, J.; Shi, A.-C.; Linse, P. *Macromolecules* **1996**, 29, 5907.  
 (42) Value was estimated by plotting  $\chi_{\text{ODT}}$  as a function of  $T_{\text{ODT}}$  for a series of symmetric diblocks and obtaining a linear fit to that data.  $(\chi N)_{\text{ODT}}$  was calculated using the BLFH prediction:<sup>25</sup>

$$(\chi N)_{\text{ODT}} = 10.495 + 41.022\bar{N}^{-1/3}$$

where  $\bar{N} = Na^6v^{-2}$ ,  $N$  is the number of statistical segment lengths,  $a$  is the statistical segment length, and  $v$  is the statistical segment volume.

- (43) Hillmyer, M. A.; Bates, F. S.; Almdal, K.; Mortensen, K.; Ryan, A. J.; Fairclough, J. P. A. *Science* **1996**, 271, 976.  
 (44) Fetters, L. J.; Lohse, D. J.; Richter, D.; Witten, T. A.; Zirkel, A. *Macromolecules* **1994**, 27, 4639.  
 (45) Turner, D. C.; Gruner, S. M. *Biochemistry* **1992**, 31, 1340.  
 (46) Gruner, S. M. *J. Chem. Phys.* **1989**, 93, 7562.  
 (47) Anderson, D. M.; Gruner, S. M.; Leibler, S. *Proc. Natl. Acad. Sci. U.S.A.* **1988**, 85, 5364.  
 (48) Sadoc, J. F.; Charvolin, J. *J. Phys. (Paris)* **1986**, 47, 683.  
 (49) Malcolm, G. N.; Rowlinson, J. S. *Trans. Faraday Soc.* **1957**, 53, 921.  
 (50) Raçon, Y.; Charvolin, J. *J. Phys. Chem.* **1988**, 92, 2646.  
 (51) Funari, S. S.; Holmes, M. C.; Tiddy, G. H. T. *J. Phys. Chem.* **1992**, 96, 11029.  
 (52) Funari, S. S.; Holmes, M. C.; Tiddy, G. J. T. *J. Phys. Chem.* **1994**, 98, 3015.  
 (53) Carvel, M.; Hall, D. G.; Lyle, I. G.; Tiddy, G. J. T. *Faraday Discuss. Chem. Soc.* **1986**, 81, 223.  
 (54) Shyamsunder, E.; Gruner, S. M.; Tate, M. W.; Turner, D. C.; So, P. T. C.; Tilcock, C. P. S. *Biochemistry* **1988**, 27, 2332.  
 (55) Mitchell, D. J.; Tiddy, G. J. T.; Waring, L.; Bostock, T.; McDonald, M. P. *J. Chem. Soc., Faraday Trans. 1* **1983**, 79, 975.  
 (56) Kagimoto, A.; Murakami, S.; Fujishiro, R. *Makromol. Chem.* **1967**, 105, 154.

- (57) Value was estimated from heats of dilution of  $C_{12}EO_m$  surfactants in water from Meguro, K.; Ueno, M.; Esumi, K. *Micelle Formation in Aqueous Media*. In *Nonionic Surfactants-Physical Chemistry*; Schick, M. J., Ed.; Marcel Dekker: New York, 1987.  
 (58) Smith, G. D.; Yoon, D. Y.; Jaffe, R. L.; Colby, R. H.; Krishnamoorti, R.; Fetters, L. J. *Macromolecules* **1996**, 29, 3462.  
 (59) Anderson, D. M.; Davis, H. T.; Scriven, L. E.; Nitsche, J. C. C. *Adv. Chem. Phys.* **1990**, 77, 337.  
 (60) Devanand, K.; Selser, J. C. *Nature* **1990**, 343, 739.  
 (61) Bailey, F. E.; Callard, R. W. *J. Appl. Polym. Sci.* **1959**, 1, 373.  
 (62) Bailey, F. E.; Kucera, J. L.; Imhof, L. G. *J. Polym. Sci.* **1958**, 22, 517.  
 (63) Ring, W.; Cantow, H.-J.; Holtrup, W. *Eur. Polym. J.* **1966**, 2, 151.  
 (64) Sadron, C.; Rempp, P. *J. Polym. Sci.* **1958**, 29, 127.  
 (65) Braun, D.; Törmälä, P. *Macromol. Chem.* **1978**, 179, 1025.  
 (66) Tasaki, K. *J. Am. Chem. Soc.* **1996**, 118, 8459.  
 (67) Callard, R. W.; Faucher, J. A. Unpublished results reported by Bailey, F.E.; Koleske, J. V. Configuration and Hydrodynamic Properties of the Polyoxyethylene Chain in Solution. In *Nonionic Surfactants-Physical Chemistry*; Schick, M. J., Ed.; Marcel Dekker: New York, 1987.  
 (68) Courval, G. J.; Gray, D. G. *Polymer* **1983**, 24, 323.  
 (69) Maron, S. H.; Filisko, F. E. *J. Macromol. Sci., Phys.* **1972**, B6 (1), 79.  
 (70) Macconachie, A.; Vasudevan, P.; Allen, G. *Polymer* **1978**, 19, 33.  
 (71) Liu, K.-J.; Parsons, J. L. *Macromolecules* **1969**, 2, 529, note that the volume ratio at which these authors identify formation of the PEO-water complex corresponds to a stoichiometry of two water molecules per EO unit, contrary to that reported in the paper.  
 (72) Maxfield, J.; Shepherd, I. W. *Polymer* **1975**, 16, 505.  
 (73) Nilsson, P.-G.; Wennerström, H.; Lindman, B. *J. Phys. Chem.* **1983**, 87, 1377.